CFD-Based Numerical Investigation and Geometric Optimization of Orifice-Induced Hydrodynamic Cavitation Reactors

M. Akrami[1], N. Naziri[2*] , A. Aliparast[3]
[1]*CFD Simulation Engineer, Research and Development Department, Azar Energy Tabriz Co., Tabriz, Iran*
[2]*Plant Manager, Azar Energy Tabriz Co., Tabriz, Iran,*
[3]*CFD Simulation Engineer, Research and Development Department, Azar Energy Tabriz Co., Tabriz, Iran*
info@azarenergy.com

Abstract
Hydrodynamic cavitation is an effective fluid dynamic mechanism for enhancing mass transfer and intensifying chemical processes, with its performance being highly sensitive to operating pressure and orifice geometry. In this study, a numerical investigation was conducted to examine the coupled effects of inlet pressure and orifice geometry on cavitation behavior in an orifice-based hydrodynamic cavitation reactor. Simulations were performed for inlet pressures of 6–10 bar, and cavitation characteristics were evaluated based on static pressure distribution and vapor volume fraction. The results indicate that increasing the inlet pressure intensifies cavitation by generating deeper pressure minima at the orifice throat and delaying downstream pressure recovery, thereby expanding the cavitating zone along the orifice wall. A strong spatial correspondence between pressure minima and vapor volume fraction peaks confirms that cavitation development is governed primarily by the local pressure field. Geometric analysis for orifice diameters of 2, 4, and 8 mm revealed that excessively small orifices induce severe pressure drops and premature bubble collapse, whereas larger orifices produce insufficient cavitation due to limited pressure reduction. An intermediate orifice diameter of 4 mm provides optimal cavitation performance, characterized by balanced pressure reduction, rapid pressure recovery, sustained vapor generation, and reduced hydraulic losses. These findings offer practical design guidelines for achieving controlled and efficient cavitation in hydrodynamic cavitation reactors.

Keywords: Hydrodynamic cavitation, Orifice-based reactor, Pressure recovery, Vapor volume fraction, CFD.

Introduction
Hydrodynamic cavitation (HC) has emerged over the past two decades as an effective process intensification (PI) technique due to its ability to enhance mass and energy transfer, generate highly reactive radical species, induce molecular fragmentation, and promote surface reactions through the high-energy collapse of vapor bubbles. As a result, HC has found widespread applications in wastewater treatment, advanced oxidation processes (AOPs), degradation of organic contaminants, emulsification, and heavy crude oil upgrading [1]. The underlying mechanism of HC involves the formation of vapor-filled cavities when a flowing liquid experiences a sudden increase in velocity accompanied by a corresponding drop in static pressure below the vapor pressure. Subsequent pressure recovery leads to rapid bubble

collapse, generating localized extreme conditions of pressure and temperature. The intensity, spatial extent, and effectiveness of this phenomenon are strongly dependent on the design of the cavitation-inducing element [2]. Among various cavitation generators, orifice plates and Venturi devices are the most commonly employed owing to their simple geometry, low manufacturing cost, and predictable hydrodynamic behavior [3]. Previous studies have demonstrated that even subtle variations in orifice geometry-including the orifice-to-pipe diameter ratio ($\beta = d/D$), plate thickness, inlet angle, and edge profile can markedly alter flow structure, pressure recovery behavior, and cavitation intensity. In general, decreasing β enhances pressure drop and cavitation intensity; however, excessive restriction or increased plate thickness may suppress bubble growth, extend the reattachment length, and reduce effective bubble collapse [4]. Despite the recognized importance of geometric effects, experimental investigation of cavitation dynamics is often constrained by high cost, limited spatial resolution, and the difficulty of measuring transient pressure and vapor structures. In this context, Computational Fluid Dynamics (CFD) has become a powerful and reliable tool for resolving the complex multiphase flow features associated with hydrodynamic cavitation. Advanced multiphase formulations, such as mixture or Euler-Euler approaches combined with established cavitation models (e.g., Schnerr-Sauer or Zwart-Gerber-Belamri), enable detailed prediction of pressure fields, vapor volume fractions, and cavitation structures under varying geometric and operating conditions [5].
Despite extensive CFD studies on hydrodynamic cavitation, a systematic assessment of the coupled effects of orifice-to-pipe diameter ratio and orifice thickness on cavitation performance remains limited, particularly from a design-oriented perspective. Accordingly, the present study aims to provide a comprehensive numerical investigation of these key geometric parameters in an orifice-based hydrodynamic cavitation reactor. Three-dimensional two-phase CFD simulations were performed using ANSYS Fluent to quantify cavitation intensity, spatial development, and pressure recovery characteristics for different orifice configurations. Numerical accuracy was ensured through a mesh-independence analysis based on the Grid Convergence Index (GCI) methodology. The findings of this work offer quantitative design guidelines for optimizing orifice geometry and improving the efficiency of industrial-scale hydrodynamic cavitation reactors [6].

Materials and Methods

The hydrodynamic cavitation flow was simulated using ANSYS Fluent with a three-dimensional, two-phase Euler-Euler approach. The Mixture model was employed for the water-vapor system, with water as the primary phase and vapor as the secondary phase. Turbulence was modeled using the Realizable k-ε model. Cavitation was captured via the Zwart-Gerber-Belamri model, assuming identical bubble radii and accounting for evaporation and condensation. Governing equations included continuity, momentum, and vapor mass transport. Boundary conditions and mesh independence were carefully tested to ensure numerical accuracy. Detailed descriptions of the multiphase and cavitation formulations can be found in [7-11].

Geometry Description

The hydrodynamic cavitation reactor was modeled as a two-dimensional axisymmetric domain with five sections: inlet pipe, converging region, orifice throat, diverging region, and outlet pipe. The key dimensions are summarized in Table 1, while Figure 1a illustrates the overall geometry. Inlet and outlet diameters were 30 mm, with axial lengths of 30 mm and 200 mm, respectively. The orifice throat length was fixed at 4 mm. Two geometric variables were studied parametrically: (1) orifice diameter (2, 4, 8 mm) and (2) entrance-edge profile (diverging angle). These variations allowed systematic assessment of their influence on flow acceleration, pressure drop, and vapor cavity distribution.

Table 1. Geometrical characteristics of the orifice

Parameter	Inlet diameter	Outlet diameter	Throat length	Upstream straight length	Downstream straight length	Throat height
unit (mm)	30	30	4	30	200	12

Mesh sensitivity was examined using three levels: coarse, medium, and fine. Key metrics including maximum velocity, volumetric flow, and cavitation number were analyzed. Mesh independence was confirmed using the Grid Convergence Index (GCI) method [12], with convergence achieved when $((GCI_{(23)})/(GCI_{(12)} \times r^p) \approx 1)$. Representative mesh distribution is shown in Figure 1b, and convergence results are summarized in Table 2.

Table 2. Mesh convergence analysis using the Roache method

Mesh	Cells	Max Velocity (m/s)	Volumetric Flow (L/min)	Cavitation Number	GCI
Coarse	15321	45.4	22.931	0.0939	1.005
Medium	21315	45.8	22.740	0.0925	0.9956
Fine	35616	45.9	22.538	0.0921	0.9941

Simulation Setup

A transient multiphase model based on the Navier–Stokes equations was employed using a homogeneous mixture approach. Flow was assumed isothermal. Turbulence was modeled via the k-ε model with standard wall functions, and cavitation was captured using the Zwart-Gerber-Belamri model. Pressure-velocity coupling used the SIMPLE algorithm, with PRESTO! for pressure discretization. Momentum equations were solved using second-order upwind, and turbulence with first-order upwind. Thermo-physical properties of the phases are listed in Table 3.

Table 3. Thermo-physical properties of phases.

Phase	Density(kg/m^3)	Viscosity(kg/m-s)
Primary phase (liquid)	998.2	0.001003
Secondary phase (vapour)	0.5542	1.34e-05

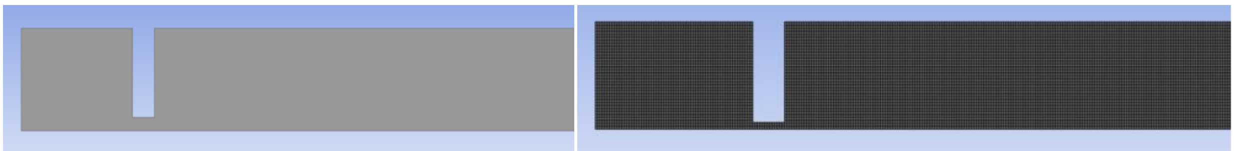

a b

Figure 1. (a) flow domain-(b) Mesh element for CFD Analysis

Results and discussion

Static Pressure and Vapor Volume Fraction Distribution

Figure 2(b) presents the axial static pressure distribution for inlet pressures of 6, 8, and 10 bar. A pronounced pressure drop is observed immediately at the orifice entrance, where the local pressure approaches or falls below the vapor pressure, indicating cavitation inception. Increasing the inlet pressure intensifies this pressure drop, leading to lower minimum pressures at the orifice throat. In addition, higher inlet pressures delay pressure recovery downstream, thereby extending the low-pressure region along the orifice wall. This hydrodynamic behavior directly governs vapor generation. As shown in Figure 2(a), regions of minimum static pressure spatially coincide with peaks in vapor volume fraction, confirming that cavitation development is primarily controlled by the local pressure field. Increasing the inlet pressure from 6 to 10 bar results in a monotonic increase in the maximum vapor volume fraction, reflecting enhanced cavitation intensity. The delayed pressure recovery sustains vapor formation over a longer axial distance, producing more stable and concentrated cavitating structures near the wall. Notably, vapor volume fraction remains negligible outside the orifice region for all inlet pressures, consistent with the full pressure recovery downstream. This confirms that cavitation is highly localized and induced predominantly by the pressure evolution imposed by the orifice geometry rather than upstream flow conditions alone. Overall, higher inlet pressures promote deeper pressure minima, delayed recovery, and expanded cavitation zones, thereby intensifying hydrodynamic cavitation within the reactor.

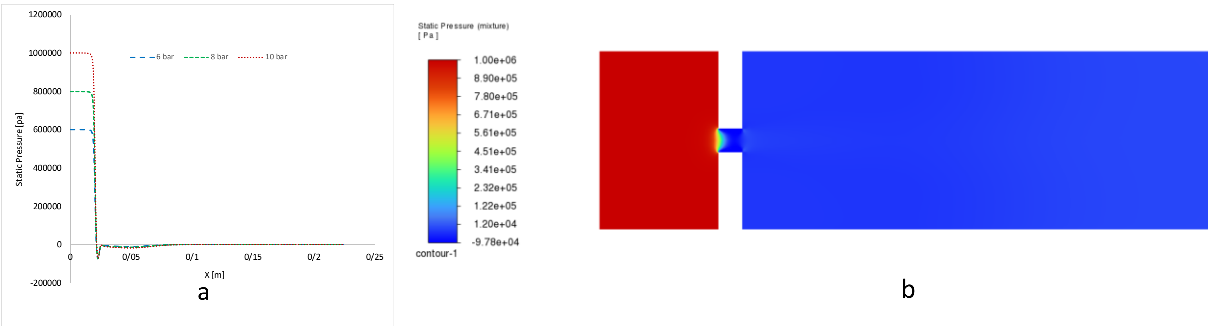

Figure 2. (a)Pressure distribution on the orifice walls at different inlet pressures 6 - 10 bar - Orifice diameter 4 mm - Orifice thickness 4 mm. (b) Static pressure contour at the orifice at different inlet pressures 10 bar

Effect of Orifice Geometry on Cavitation Characteristics

The influence of orifice geometry was investigated by varying both the entrance-edge profile and the orifice diameter. Velocity contours (Figure 3) show that a divergent (beveled) orifice effectively suppresses flow separation compared to a straight-cut configuration, leading to a more stable downstream flow field. However, vapor volume fraction contours reveal that a moderate divergent angle (8°) enhances cavitation intensity, producing higher vapor concentrations near the orifice wall. Beyond this angle, cavitation intensity decreases due to reduced local pressure gradients. The axial pressure distributions for different orifice diameters (2, 4, and 8 mm) further illustrate the geometric influence on cavitation. All configurations exhibit a sharp pressure drop at the throat, triggering vapor formation. Larger diameters (higher β ratios) generate more extended low-pressure regions, increasing bubble residence time within the cavitation zone. This behavior highlights the strong dependence of cavitation development on pressure recovery characteristics rather than solely on the magnitude of the pressure drop.

Evaluation of Orifice Diameter Based on Bubble Dynamics and Pressure Recovery

Figure 4 illustrates the variation of bubble diameter and pressure ratio as a function of dimensionless time for different orifice diameters [12]. The results indicate that changes in orifice diameter moderately affect the maximum bubble size, while exerting a strong influence on bubble lifetime. Larger diameters (higher β ratios) lead to prolonged bubble persistence due to smoother pressure recovery, whereas smaller diameters promote rapid pressure fluctuations that accelerate bubble collapse. This behavior highlights the dominant role of pressure recovery characteristics in governing cavitation dynamics rather than the peak pressure drop alone. The pressure recovery behavior obtained from CFD simulations at an inlet pressure of 10 bar is compared for different orifice diameters in Figure 5. The 2 mm orifice exhibits an excessive pressure drop followed by delayed recovery, which induces flow choking and premature collapse of vapor structures. In contrast, the 8 mm orifice shows a milder pressure reduction and rapid recovery, resulting in weaker cavitation development. The 4 mm configuration provides a balanced pressure profile, characterized by sufficient pressure depression for cavitation inception and a controlled recovery that sustains vapor formation over an extended axial distance. Quantitative comparison of cavitation performance parameters at 10 bar is summarized in Table 4. Although the 2 mm orifice produces the highest local velocities, it suffers from excessive hydraulic losses and reduced vapor stability. The 8 mm orifice yields lower vapor volume fractions due to insufficient pressure reduction. The 4 mm orifice achieves an optimal compromise, combining favorable vapor volume fraction, moderate maximum velocity, and a lower cavitation number. These findings confirm that an intermediate orifice diameter offers the most effective and controllable cavitation performance under the investigated operating conditions.

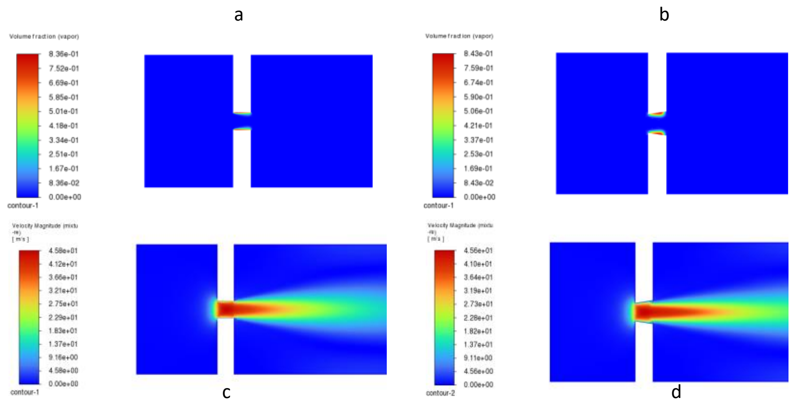

Figure 3. (a) Vapor volume fraction contour for orifice mode with straight cross-sectional geometry, (b) Vapor volume fraction contour for 8 degree orifice mode, (c) Velocity contour for the orifice case with straight cross-section geometry, (d) Velocity contour for the orifice case with angle

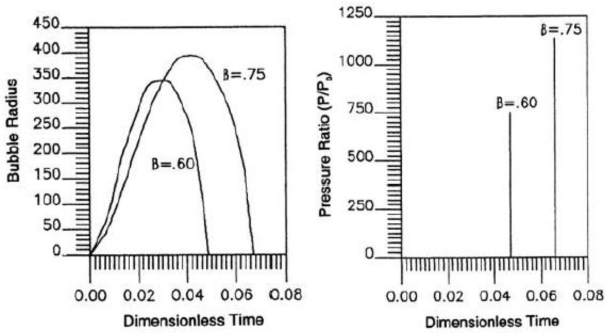

Figure 4. Bubble diameter size and pressure ratio in dimensionless time and the effect of different diameters[12]

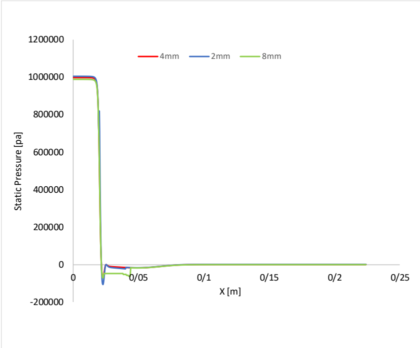

Figure 5. Comparison of pressure recovery at different orifice diameters at 10 bar pressure

Table 4. Comparison of important parameters in different diameters

Pressure inlet D=2mm	Max Velocity (m/s)	Volum fraction (vapor)	Cavitation Number
10 bar	45.2	0.705	1.0046
Pressure inlet D=4mm	Max Velocity (m/s)	Volum fraction (vapor)	Cavitation Number
10 bar	45.8	0.836	0.9956
Pressure inlet D=8mm	Max Velocity (m/s)	Volum fraction (vapor)	Cavitation Number
10 bar	46.3	0.936	0.9912

Conclusions

A CFD-based numerical investigation was conducted to elucidate the effects of inlet pressure and orifice geometry on cavitation behavior in an orifice-based reactor. The results demonstrated that increasing inlet pressure intensifies cavitation by generating deeper pressure minima at the orifice throat and delaying downstream pressure recovery, thereby expanding the low-pressure region and increasing vapor volume fraction. A strong spatial correlation between static pressure minima and vapor volume fraction peaks confirmed that cavitation inception and development are primarily governed by the local pressure field. Orifice geometry was shown to play a crucial role in both flow stability and cavitation intensity. While a divergent beveled orifice suppresses flow separation and stabilizes the downstream flow, it enhances cavitation only up to an optimal divergence angle, indicating a trade-off between hydrodynamic stability and cavitation performance. Moreover, the orifice-to-pipe diameter ratio (β) was identified as a key design parameter. Small diameters caused excessive pressure drops and premature bubble collapse, whereas large diameters produced insufficient cavitation. An intermediate diameter of 4 mm provided the most favorable performance, characterized by balanced pressure reduction, rapid recovery, sustained vapor generation, and reduced hydraulic losses. Overall, this study provides practical design guidelines for optimizing hydrodynamic cavitation reactors through appropriate selection of inlet pressure and orifice geometry, enabling controlled and efficient cavitation for engineering applications.

Acknowledgements

The authors gratefully acknowledge Azar Energy Tabriz Company for providing the necessary facilities and technical support to conduct this research at its Research and Development (R&D) unit. The authors also thank their colleagues for their valuable cooperation and contributions during the course of this study.

References

[1] Chen, Y., C. Yin, and Y. Song, Application of hydrodynamic cavitation in the field of water treatment. Chemical Papers, 2023. **77**(7): p. 3521-3546.

[2] Panda, D., V.K. Saharan, and S. Manickam, Controlled hydrodynamic cavitation: A review of recent advances and perspectives for greener processing. Processes, 2020. **8**(2): p. 220.

[3] Roy, S., et al., Numerical modelling and experimental validation of an orifice plate-based hydrodynamic cavitation process for improving the biomass pretreatment. Biotechnology Reports, 2025: p. e00925.

[4] Davoudi, M.R. and M. Mahdi, Experimental and numerical investigation of geometric effect on cavitation flow through orifice. Mechanics & Industry, 2021. **22**: p. 31.

[5] Pietrykowski, K. and P. Karpiński, Simulation study of hydrodynamic cavitation in the orifice flow. Applied Computer Science, 2022. **18**(3): p. 31-41.

[6] Ji, C., Z. He, and Y. Zhixia. Experimental and numerical investigation on the performance of hydrodynamic cavitation in multi-holes orifice plate. in 3rd International Conference on Material, Mechanical and Manufacturing Engineering (IC3ME 2015). 2015. Atlantis Press.

[7] Dular, M., et al., Scale effect on unsteady cloud cavitation. Experiments in fluids, 2012. **53**(5): p. 1233-1250.

[8] Sommerfeld, M., Numerical methods for dispersed multiphase flows, in Particles in flows. 2017, Springer. p. 327-396.

[9] Manninen, M., V. Taivassalo, and S. Kallio, On the mixture model for multiphase flow. 1996.

[10] Garcia-Villalba, M., et al., Numerical methods for multiphase flows. International Journal of Multiphase Flow, 2025: p. 105285.

[11] Zwart, P.J., A.G. Gerber, and T. Belamri. A two-phase flow model for predicting cavitation dynamics. in Fifth International Conference on Multiphase Flow.–Yokohama, Japan.–2004. 2004.

[12] Shah, Y.T., A. Pandit, and V. Moholkar, Cavitation reaction engineering. 1999: Springer Science & Business Media.